Spectral statistics and scattering resonances of complex primes arrays

Ren Wang, Felipe A. Pinheiro, and Luca Dal Negro

Phys. Rev. B **97**, 024202 — Published 16 January 2018

DOI: 10.1103/PhysRevB.97.024202

Spectral Statistics and Scattering Resonances of Complex Primes Arrays

Ren Wang[1], Felipe A. Pinheiro[2], Luca Dal Negro[1,3,4*]

1. *Department of Electrical and Computer Engineering, Boston University, Boston, MA 02215, USA*
2. *Instituto de Fisica, Universidade Federal do Rio de Janeiro, Rio de Janeiro-RJ 21941-972, Brazil*
3. *Division of Material Science and Engineering, Boston University, Boston, MA 02215, USA*
4. *Department of Physics, Boston University, Boston, MA 02215, USA*

(Dated: January 3, 2018)

We introduce a novel class of aperiodic arrays of electric dipoles generated from the distribution of prime numbers in complex quadratic fields (Eisenstein and Gaussian primes) as well as quaternion primes (Hurwitz and Lifschitz primes), and study the nature of their scattering resonances using the vectorial Green's matrix method. In these systems we demonstrate several distinctive spectral properties, such as the absence of level repulsion in the strongly scattering regime, critical statistics of level spacings, and the existence of critical modes, which are extended fractal modes with long lifetimes not supported by either random or periodic systems. Moreover, we show that one can predict important physical properties, such as the existence spectral gaps, by analyzing the eigenvalue distribution of the Green's matrix of the arrays in the complex plane. Our results unveil the importance of aperiodic correlations in prime number arrays for the engineering of novel gapped photonic media that support far richer mode localization and spectral properties compared to usual periodic and random media.

INTRODUCTION

The study of classical and quantum waves in complex and disordered scattering media unveiled fascinating analogies between the behavior of electronic and optical wave excitations [1]. Anderson localization of light [2], which leads to a breakdown of wave propagation in strongly scattering media, is probably the best known example. However, the applications of random media to optical engineering are presently quite limited due to the lack of simple design rules for deterministic optimization. As an alternative, aperiodic optical media, including quasi-periodic crystals constructed by following deterministic mathematical rules [3], recently attracted significant interest in the optics and electronics communities because of their simplicity in design and fabrication, as well as compatibility with current material deposition and device fabrication technologies [4–10]. In particular, a substantial amount of recent experimental and theoretical studies in the fields of nanophotonics, plasmonics and metamaterials have focused on understanding structure-property relationships in complex media with aperiodic order for the demonstration of novel optical functionalities [11–18]. Deterministic aperiodic structures support distinctive optical properties that are absent in either periodic or random systems, such as fractal mode spectra with controllable anomalous transport behavior [19–22], and a rich spectrum of optical modes that show various degrees of spatial localization, known as critical modes [23–25]. Critical modes feature highly fragmented multi-fractal envelopes with a power-law decay that found recent applications in aperiodic lasing, optical sensing, photo-detection, and nonlinear optical devices [10, 16, 26–28]. Moreover, topologically protected edge-states were recently discovered in the pseudo-gap spectra of quasicrystals [29–31], significantly broadening our understanding of topological phases in optical media. However, the vast majority of previous studies focused on quasicrystalline structures that are constructed by local matching rules, such as the Penrose lattice, or on deterministic scattering arrays generated by binary inflation rules, of which the Fibonacci, Thue-Morse, and Rudin-Shapiro sequences are the primary examples [19, 26, 29–35].

In this paper, based on the distinctive aperiodic distribution of prime numbers in complex quadratic fields and quaternion rings, referred to as Complex Primes Arrays (CPAs), we introduce a new class of highly-diffractive arrays with non-crystallographic rotational symmetries, i.e., structures characterized by spatial Fourier spectra that support countably infinite discrete components. These structures exhibit a rich interplay between structural regularity, both at the local level and long-range, and unpredictability in the distribution of prime numbers that has roots in the most fundamental questions of number theory [36, 37]. Remarkably, Fourier spectral methods applied to the prime number distribution unveiled a noise spectrum with self-similarity described by a power-law scaling [38]. This behavior characterizes self-organized critical states of dynamical systems that do not possess any characteristic length scale [39].

Here we apply the vector Green' s matrix method, which has been extensively utilized for the the study of scattering resonances in open random media [40–46], to a comprehensive investigation of the spectral statistics of scattering resonances in CPAs of electric dipoles, namely the Eisenstein, Gaussian, Hurwitz, and Lifschitz prime arrays. Specifically in these structures we systematically study the diffraction spectra, the eigenvalue distribution of the Green's matrix, the Density of States, the level spacing distribution, the decay rate statistics, and the spatial extent of the supported eigenmodes. By means

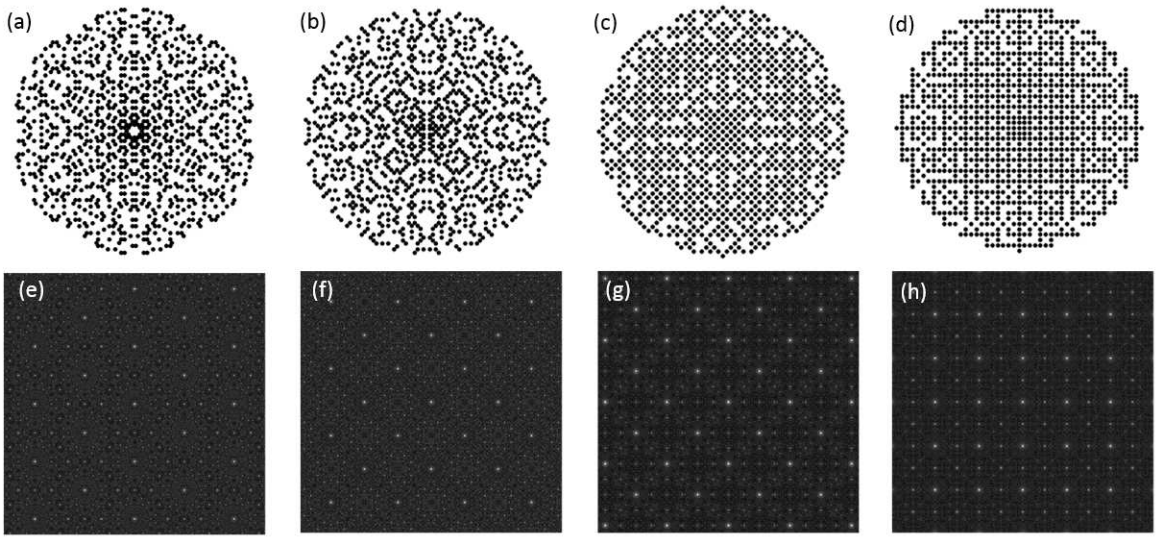

FIG. 1. (a) N = 1050 Eisenstein prime array, (b) N = 1068 Gaussian prime array, (c) N = 1093 Hurwitz prime array, and (d) N = 1081 Lifschitz prime array. (e) to (h) are the diffraction patterns (5th root taken to enhance contrast) of the corresponding array on top of each panel.

of extensive numerical calculations of large-scale arrays we demonstrate several unique spectral properties, such as the absence of level repulsion in the strongly scattering regime, critical level spacing statistics, and the existence of critical modes, i.e, extended fractal modes with long lifetime. In addition, we show that one can make predictions about the the existence of spectral gaps in CPAs solely by analyzing the eigenvalue distribution of the Green's matrix in the complex plane. This work introduces novel gapped photonic media with far richer localization and spectral properties compared to usual periodic and random structures.

Our paper is organized as follows. In the first section the structural properties of CPAs are analyzed whereas the spectra of the Green's matrix that describe light propagation in such structures is discussed in the second section. Level statistics and the spatial properties of the eigenmodes are treated in third and fourth sections, respectively. The last section draws our conclusion.

THE STRUCTURE OF COMPLEX PRIMES ARRAYS

The aperiodic CPAs structures considered in this work are constructed based on extensions of the familiar prime number concept from the natural integers to the complex plane, where particles coordinates are made to correspond to the real and imaginary parts of complex primes. Specifically, we focus on the prime elements of complex quadratic fields such as the Eisenstein and Gaussian integers as well as on the irreducible elements of Hurwitz and Lifschitz quaternions. Eisenstein integers are complex numbers of the form $a+b\omega$, where a and b are natural integers and $\omega = (-1 + i\sqrt{3})/2$ is one of the cubic roots of one (i is the imaginary unit). Eisenstein integers are members of the imaginary quadratic field $\mathbb{Q}(\sqrt{-3})$ which is a commutative ring often denoted $\mathbb{Z}[\omega]$. The field of Eisenstein integers has six units, namely ± 1, $\pm\omega$, and $\pm\omega^2$, which when multiplied by prime elements form the so-called prime associates (i.e., equivalent primes). Gaussian integers are complex numbers of the form $a+bi$ where a and b are integers. They are members of the imaginary quadratic field $\mathbb{Q}(\sqrt{-1})$ and form a ring often denoted $\mathbb{Z}[i]$ with units ± 1 and $\pm i$. The Eisenstein integers form a triangular lattice in the complex plane while the Gaussian integers form a square lattice.

It is known from algebraic number theory that Eisenstein and Gaussian integers are also unique factorization domains (UFDs) in which every non-zero and non-unit element can be written as a product of prime elements (or irreducible elements), uniquely up to rearrangement, complex conjugation and associates (i.e., unit multiples), analogously to the fundamental theorem of arithmetic for the natural integers. Simple characterizations can be utilized to construct Eisenstein and Gaussian prime arrays. In particular, an Eisenstein integer $a + b\omega$ is an Eisenstein prime if and only if either of the following mutually exclusive conditions hold: (i) z is equal to the product of a unit and a natural prime of the form $3n - 1$; (ii) $|z|^2 = a^2 + ab + b^2$ is a natural prime. Similarly, a Gaussian integer $a + bi$ is a Gaussian prime when (i) one of a, b is zero and the absolute value of the other is a prime number of the form $4n + 3$; (ii) both are nonzero and

$a^2 + b^2$ is a prime number.

A number of unsolved problems and conjectures are related to the aperiodic distributions of Eisenstein and Gaussian primes in the complex plane and to the nature of percolation on primes in imaginary quadratic fields [47, 48].

We will now discuss in more detail the structural properties of the proposed CPAs. Figures 1(a) and 1(b) show a representative Eisenstein prime array with $N = 1050$ elements and a representative Gaussian prime array with $N = 1068$ elements. Since multiplication by a unit and complex conjugation both preserve primality, the arrays exhibit characteristic $6\times2 = 12$ fold rotational symmetry and $2\times2 = 8$ fold symmetry, which are incompatible with translational symmetry (i.e., crystallographically forbidden). Moreover, the arrays display a regular structure that nevertheless coexists with their complete lack of periodicity. The unique interplay between symmetry and aperiodicity in these systems is captured by a rigorous result recently established by Tao [49].

A second class of CPAs can be constructed based on two-dimensional cross-sections of the irreducible elements of quaternions. Quaternions are numbers of the form $z = a + bi + cj + dk = (a, b, c, d)$ where j, j, k are symbols satisfying $i^2 = j^2 = k^2 = ijk = -1$. Integer quaternions form a noncommutative ring that unfortunately fails to be a unique factorization domain. However, Hurwitz [50] realized that one can obtain a Euclidean domain when including half units, and defined the Hurwitz integers as quaternions of the form $(a, b, c, d) \in \mathbb{Z}^4 + 1/2(1, 1, 1, 1)$ with integer Euclidean norm $N(z)$. Therefore, Hurwitz quaternions (or Hurwitz integers) are quaternions whose components are either all integers or all half-integers. Moreover, Hurwitz primes are a subset of Hurwitz quaternions with an Euclidean norm ($N(z) = a^2 + b^2 + c^2 + d^2$) that is equal to an integer prime number. Furthermore, the prime elements of the half-integers Hurwitz quaternions are referred to as Lipschitz primes. Geometrically, Hurwitz and Lipschitz integers can be viewed as the integer and the half-integer lattice points on a sphere of radius $\sqrt{N(z)}$ in $\mathbb{R}^4$. A two-dimensional section of the Hurwitz primes is shown in Fig. 1(c), consisting of the 1093-element array obtained by projecting Hurwitz primes into the complex plane (considering only the coordinates a and b of each Hurwitz primes and associating the real and imaginary components with the Cartesian coordinates of the scattering dipoles). Similarly, a Lifschitz prime array is shown in Fig. 1(d) where only the subset of Hurwitz primes with integer coordinates have been considered [51].

In order to more rigorously characterize the diffraction properties of the CPAs we studied their spatial Fourier spectra, which are obtained by computing the structure factor, shown in Figs. 1 (e-h), computed as [52]:

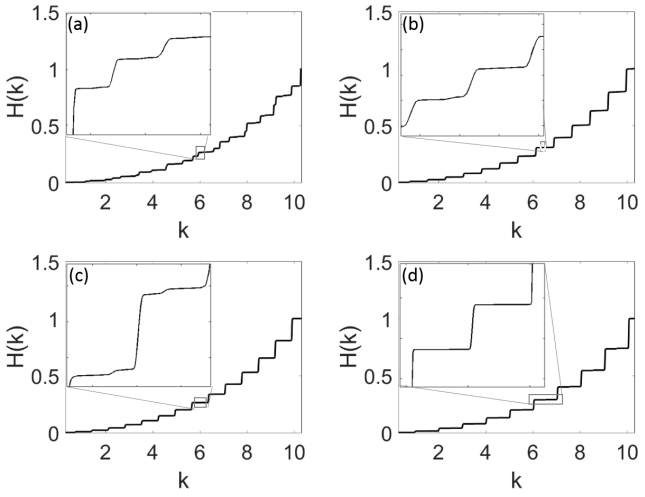

FIG. 2. The H(k) of (a) Eisenstein prime, (b) Gaussian prime, (c) Hurwitz prime, (d) Lifschitz prime.

$$S_N(\mathbf{k}) = \frac{1}{N}\sum_{n=1}^{N}\sum_{m=1}^{N} e^{-j\mathbf{k}\cdot(\mathbf{r}_n-\mathbf{r}_m)} \qquad (1)$$

where N is the total number of particles in the array. The high degree of structural regularity of the CPAs is manifested in the rotational symmetry of the spectra in Figs. 1 (e-h), which is a consequence of the corresponding number of associates, as well as in the presence of sharp diffraction peaks. At a closer inspection, these diffraction patterns reveal a hierarchical structure that encodes spatial correlations at multiple length scales. A similar behavior occurs in traditional quasicrystals, e.g. the Penrose lattice, where highly diffractive Bragg peaks densely fill the reciprocal space in a non-periodic and self-similar fashion. However, in addition to singular components (i.e., sharp diffraction peaks) in the diffraction spectra, we also notice in Figs. 1 (e-h) the presence of a weaker continuous component, or a diffuse background that is typically associated to structural disorder in complex media. This is particularly evident for the Eisenstein prime array in Fig. 1 (e) and for the Gaussian prime array in Fig. 1 (f), whose structures are more complex than the ones of Hurwitz and Lifschitz prime arrays shown in Figs. 1 (g,h), respectively. Aperiodic structures whose diffraction spectra display a coexistence of singular and continuous spectral components are referred to as singular-continuous, and our numerical results provide evidence that the proposed CPAs belong to this category. Singular-continuous spectra are often discovered in complex systems with chaotic dynamics, fractal structures, and are commonly observed in traditional quasicrystals [3]. Singular continuous spectra are often associated to multi-fractal systems. Due to their long-range correlated nature, the investigated CPAs fea-

ture a characteristic size-dependence mostly attributed to the continuous component of their spectra. However, as the size of the arrays is increased from few hundred particles, their spectral features are already very stable and robust with respect to size scaling. In particular, the physical properties of CPAs demonstrated in our paper for systems with approximately $N = 1000$ particles remain qualitatively unchanged as N is increased.

The nature of the Fourier spectra of CPAs can be more accurately understood by studying the behavior of the Integrated Intensity Function (IIF) [53]:

$$H_N(k) = \int_0^k \int_0^k |S_N(k'_x, k'_y)| dk'_x dk'_y \qquad (2)$$

For two-dimensional arrays this function characterizes the distribution of the diffracted intensity peaks contained within a 2D square region, centered at the origin, with maximum size $2k \times 2k$ in the reciprocal space. It should be realized that the exact nature of the diffraction spectrum is only determined by the asymptotic limit of equation (2) for a system of infinite size ($N \to \infty$) and only heuristic information can be extracted for finite-size structures. The behavior of the IIF can be understood as follows. In both periodic and quasiperiodic structures there are regions where $H(k)$ vanishes due to the discrete nature of their spectra. Therefore, over those regions $H(k)$ must remain constant and it will present jump discontinuities every time an isolated Bragg peak is integrated. On the other hand, for structures with continuous Fourier spectra the function $H(k)$ is smooth (i.e. continuous and differentiable). In the case of structures with singular-continuous spectra the Bragg peaks are no longer well-separated but cluster into a hierarchy of self-similar contributions giving rise to a continuous component in the spectrum that smoothly increases the value of $H(k)$ in between the plateaus.

In Fig. 2 we show the calculated $H(k)$ for each of the CPAs. The results demonstrate a characteristic aperiodic staircase with a fractal behavior highlighted by computing $H(k)$ over a much smaller scale, as shown in the insets of Figure 2. In Fig. 2(a) we show the $H(k)$ of the Eisenstein prime array, which demonstrates clear jump discontinuities in correspondence of the bright diffraction peaks shown in Fig. 1(e). Moreover, the presence of the continuous components is manifested by the varying slopes that smoothly connect each plateau of $H(k)$, unveiling the singular-continuous nature of the spectra. Qualitatively similar features are also observed for all the other CPAs. However, the respective contribution of the continuous components weaken progressively from Eisenstein and Gaussian primes, shown in Figs. 2(a,b), to Hurwitz and Lifschitz structures shown in Figs. 2(c,d). This behavior is consistent with the much more regular structure displayed in real space by the Hurwitz and Lifschitz arrays. Our heuristic analysis leads to conjecture a surprising connection between the distribution of primes in complex quadratic fields and the singular-continuous spectra of two-dimensional quasicrystals. We can regard this scenario as a two-dimensional generalization of Freeman Dyson's conjecture on the quasi-crystalline nature of the the Fourier spectrum of the zeta-function zeros on the critical line, which encode information on the distribution of the natural prime numbers [54].

GREEN'S MATRIX SPECTRAL PROPERTIES

The Green's matrix method is a powerful approach to study wave propagation in random media. The method relies on the analysis of the spectra of the Green's matrix, which belongs to the important class of the so-called Euclidean random matrices that appear in Random Matrix Theory (RMT) [46, 55]. The elements of a Euclidean random matrix are determined by a function of the positions of pairs of randomly distributed points in Euclidean space. The interest on non-Hermitian random matrices such as the Green's matrix has significantly increased in recent years due their applications in the theoretical description of open systems. When applied to random media, the study of the spectra of Green's matrices unveiled important information about scattering resonances [40, 41, 46]. Moreover, an analytical theory has also been developed for the eigenvalue density of random Green's matrices, providing fundamental insights into light-matter interactions in disordered media [46]. However, the applications of the Green's matrix method has been mostly restricted to random media so far. Recently, we have applied this approach to deterministic aperiodic arrays ranging from quasiperiodic to pseudo-random and shed some light on the distinctive structure-property relationships that govern the optical behavior of large systems of scattering particles with controllable degree of aperiodic order [52, 56].

The vectorial Green's matrix method describes light propagation in a medium composed of identical, point-like dipoles arbitrarily positioned inside a homogeneous background medium (typically in vacuum). The elements of the $3N \times 3N$ Green's matrix follow from the general electromagnetic dyadic Green's function calculated based on the relative positions of the N dipoles as [57]:

$$\mathbf{G}_{nm}(k, \mathbf{r}_{nm}) = \begin{cases} -\frac{\exp(ikr_{nm})}{i4\pi r_{nm}} \left\{ [\mathbf{U} - \widehat{\mathbf{r}}_{nm}\widehat{\mathbf{r}}_{nm}] - \left(\frac{1}{ikr_{nm}} + \frac{1}{(kr_{nm})^2} \right) [\mathbf{U} - 3\widehat{\mathbf{r}}_{nm}\widehat{\mathbf{r}}_{nm}] \right\} & \text{for} \quad n \neq m \\ 0 & \text{for} \quad n = m, \end{cases} \qquad (3)$$

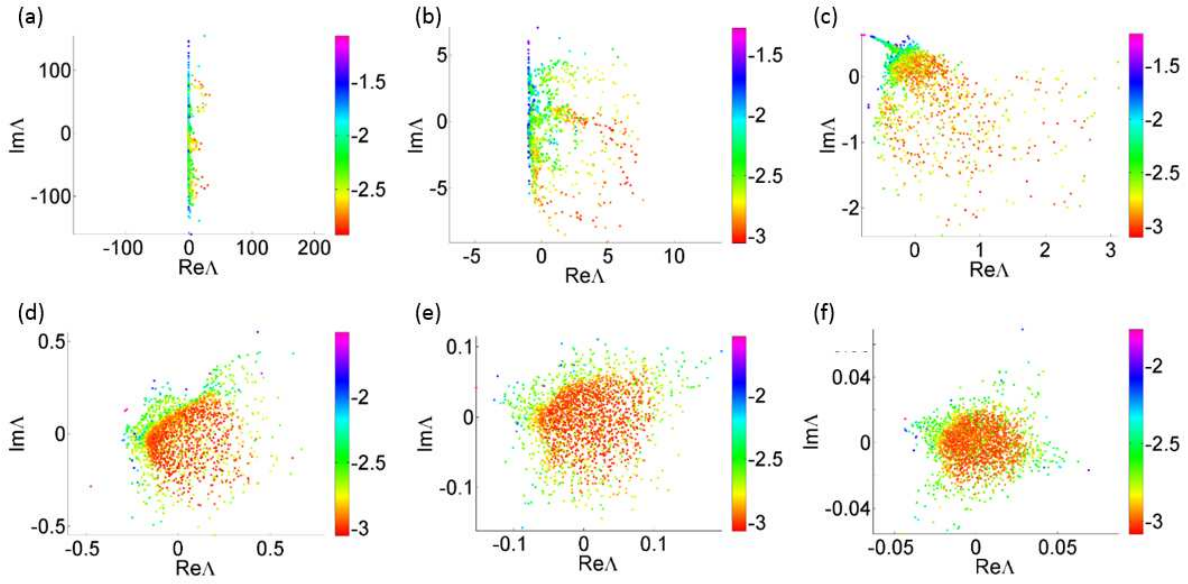

FIG. 3. (Color online) Eigenvalue distributions of Eisenstein prime arrays with $\rho\lambda^2$ = (a) 100, (b) 10, (c) 1, (d) 0.1, (e) 0.01, (f) 0.001. The color-coding shows the log_{10} values of IPR for the eigenmode corresponding to each eigenvalue.

where $\mathbf{G}_{nm}$ is the 3×3 block element of the dyadic Green's matrix, integer indices for particles $n, m \in 1, 2, 3, ..., N$, k is the wavenumber, U is a 3×3 identity matrix, $\hat{\mathbf{r}}_{nm}$ is the vectorial position from the nth to mth particle, and its magnitude is r.

By studying the distribution of complex eigenvalues Λ of Green's matrix in the complex plane, important physical information on the scattering system can be extracted. In fact, it has been established that the real and imaginary parts of Λ are approximately equal to the relative widths $(\Gamma - \Gamma_0)/\Gamma_0$ and frequency $(E - E_0)/\Gamma_0$ of the scattering resonances of a scattering system, respectively [40].

In Figs. 3 and 4 we show the eigenvalue distributions for different values of the optical density $\rho\lambda^2$ (with ρ the number of particles per unit area and λ the optical wavelength) for Eisenstein prime and Hurwitz prime arrays, respectively. Qualitatively similar results are also obtained for Gaussian primes and Lifschitz structures, which are shown in the Supplemental Material Fig. S1 and S2 [58].

All the complex eigenvalues shown in Figs. 3 and 4 are color-coded based on the log_{10} value of Inverse Participation Ratio (IPR) of the corresponding eigenvectors, defined as [46]:

$$IPR_p = \frac{\sum_{i=1}^{N} |\mathbf{R}_p(\mathbf{r}_i)|^4}{[\sum_{i=1}^{N} |\mathbf{R}_p(\mathbf{r}_i)|^2]^2}, \tag{4}$$

where $\mathbf{R}_p$ is the p-th eigenvector of the Green's matrix, and $\mathbf{r}_i$ are N scatterers' positions. The IPR measures the degree of spatial localization of the eigenvectors. An eigenvector that extends over all the N scatterers is characterized by a low value of $IPR \simeq 1/N$, while an eigenvector localized at a single point has $IPR = 1$. We notice in Fig. 3(a) that when the optical density is the largest (i.e. $\rho\lambda^2 = 100$), the spectrum collapses around the region $Re\Lambda = -1$ which correspond to long-lived modes (i. e., the decay rate $\Gamma \approx 0$). Furthermore, we observe that the corresponding eigenstates display larger IPR values, *i.e.* more spatial localization, towards larger values of $|Im\Lambda|$. Among the eigenvalues with $Re\Lambda \simeq -1$, those with larger absolute values in the imaginary part have increasingly higher IPR values. In random systems proximity resonances ($Re\Lambda \approx -1$, $Im\Lambda \gg 1$, and $IPR = 0.5$) spatially localized over pairs of particles very close together, may exist even for weakly scattering systems, far from the regime of Anderson localization [40]. In contrast, two-particle proximity resonances are generally absent in the investigated aperiodic systems, where eigenstates localized over small clusters of particles, similar to Efimov-type of resonances, occur more frequently due to locally symmetric particle clusters distributed across these structures. It is also interesting to notice in Fig. 3(a) that a spectral gap opens in the complex plane between $Im\Lambda = 0$ and 100. This feature, which does not occur in random arrays, reflects the role of spatial correlations in the Eisenstein prime array, and can also be observed in all the other aperiodic arrays at large enough density.

On the other hand, when the optical density decreases the sub-radiant eigenmodes at $Re\Lambda \approx -1$ gradually disappear from the spectra as shown in Figs. 3(b) to 3(f) and the complex eigenvalue distributions eventually

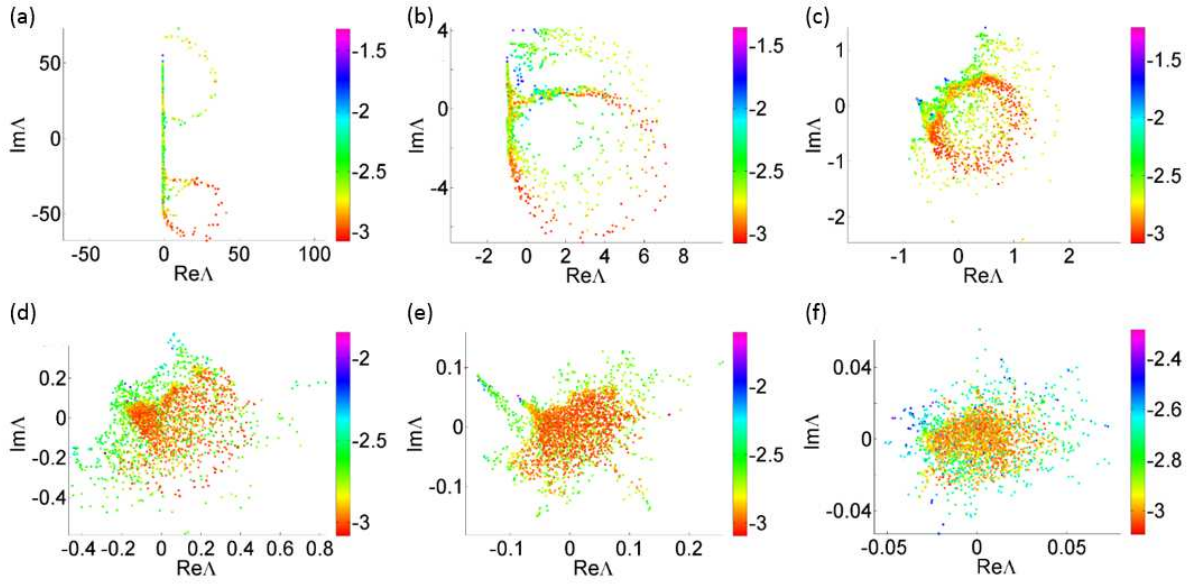

FIG. 4. (Color online) Eigenvalue distributions of Hurwitz prime arrays with $\rho\lambda^2$ = (a) 100, (b) 10, (c) 1, (d) 0.1, (e) 0.01, (f) 0.001. The color-coding shows the log_{10} values of IPR for the eigenmode corresponding to each eigenvalue.

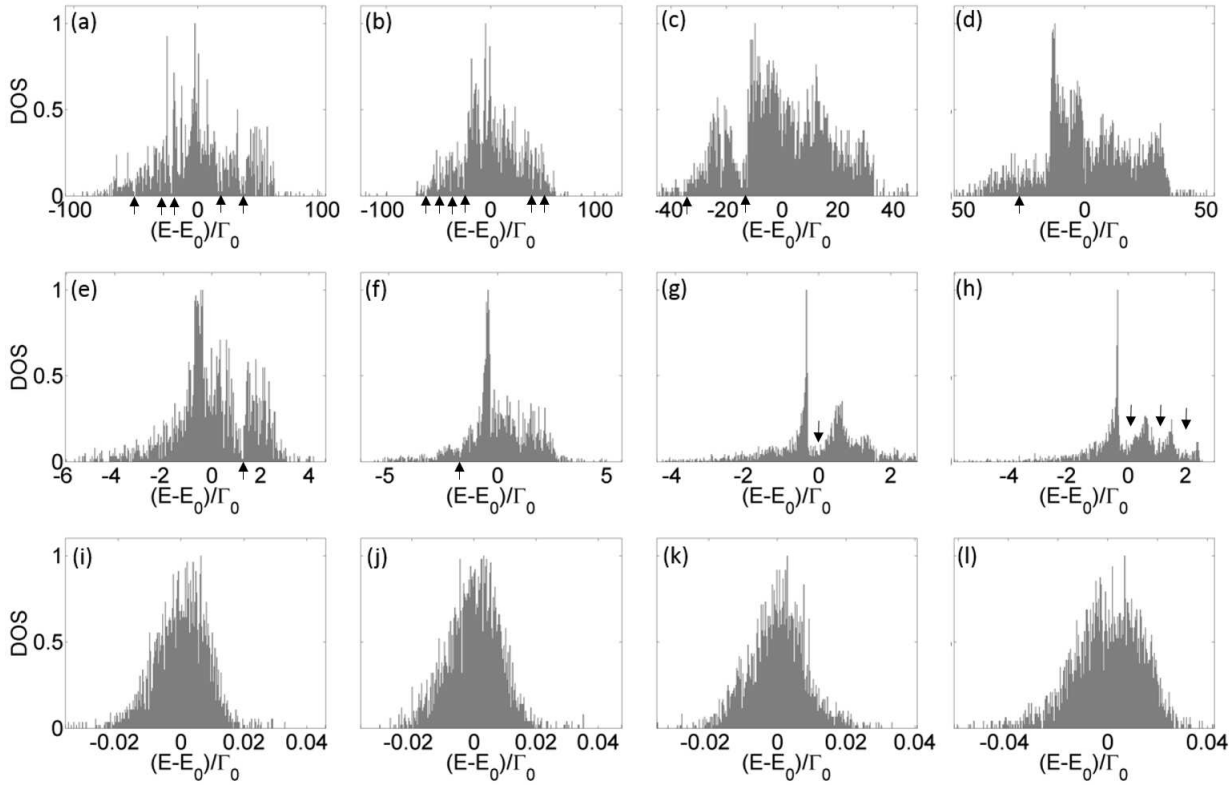

FIG. 5. The DOS for (a) Eisenstein prime, (b) Gaussian prime, (c) Hurwitz prime, (d) Lifschitz prime, at $\rho\lambda^2$=100; (e) Eisenstein prime, (f) Gaussian prime, (g) Hurwitz prime, (h) Lifschitz prime, at $\rho\lambda^2$=10.(i) Eisenstein prime, (j) Gaussian prime, (k) Hurwitz prime, (l) Lifschitz prime, at $\rho\lambda^2$=0.001.The arrows indicate the presence of spectral gaps in the DOS.

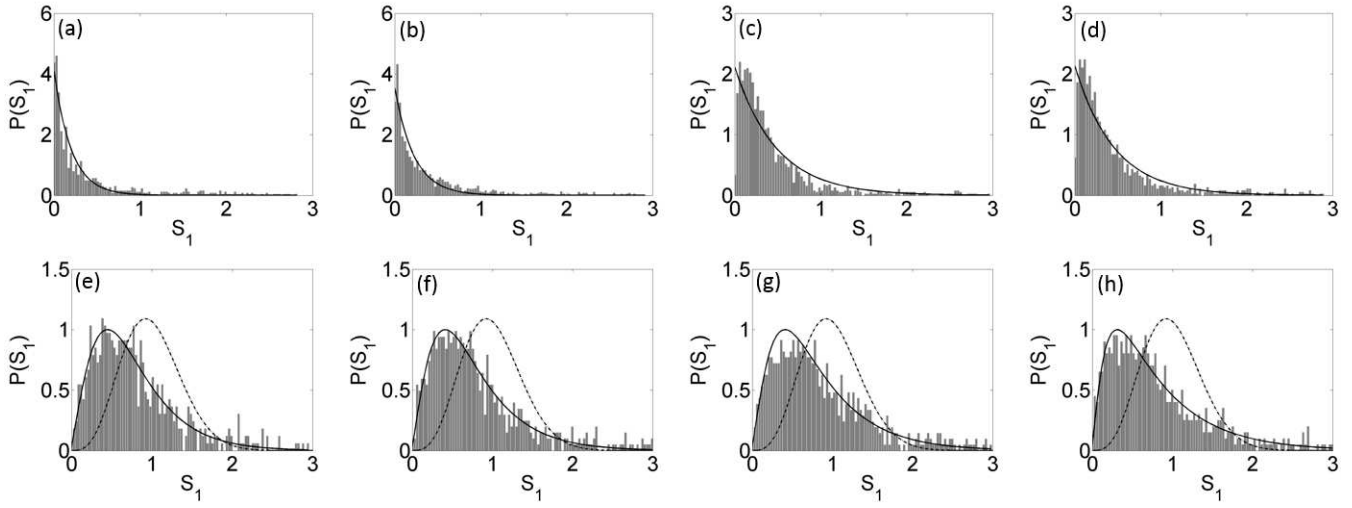

FIG. 6. The 1st-neighbor level statistics of complex eigenvalues for (a) Eisenstein prime, (b) Gaussian prime, (c) Hurwitz prime, (d) Lifschitz prime, at $\rho\lambda^2$=100; (e) Eisenstein prime, (f) Gaussian prime, (g) Hurwitz prime, (h) Lifschitz prime, at $\rho\lambda^2$=0.001. The fittings are Poissionian for (a)-(d), as well as Ginibre (dashed curve in (e)-(h)) and critical (solid curve in (e)-(h)) distributions. The mean-square error (MSE) of fittings is less than 0.01.

evolve into a more homogeneous domain in the complex plane centered near $\Lambda = 0$ (Fig. 3(d) to (f)). This spectral evolution reflects the occurrence of an increasing proportion of short-lived eigenstates with low IPR extending over a larger number of particles and characterized by a larger decay rate. Besides, the IPR values are more uniformly distributed across the different eigenvalues at low optical densities showing that these states are very similar in both energy and decay characteristics. Importantly, the low-density distribution of eigenvalues for all the investigated CPAs does not approach a circular distribution in the complex plane, as it would be the case for a uniform random medium [40, 45, 46, 52], even at very low optical density of 0.001 particle per λ^2. This indicates a persistent correlation effect, which is present even at very small optical densities, where the average interparticle separation is more than one order of magnitude larger compared than the wavelength.

In Figs. 4(a) to 4(f), we summarize the evolution of eigenvalue distributions at the six representative optical densities for a N = 1093 Hurwitz prime array. Unlike in the case of Eisenstein prime array, the distribution of eigenvalues for the Hurwitz prime array at $\rho\lambda^2 = 100$ does not feature large sub-radiant components, and it exhibits two large circular gap regions in the high-density spectrum that originates from its more significant structural regularity. This behavior is very similar to the eigenvalue distribution of a periodic square array at such large optical density (see Fig. S3 of Supplemental Material [58]). As the optical density decreases from Figs. 4(b) to 4(f), the eigenvalues eventually cluster into a smaller region of the complex plane around $\Lambda = 0$. Similar to the case of the Eisenstein prime array, the presence of correlation effects prevent the eigenvalue distribution to approach, even at the smallest density values, the circular disk distribution expected for uniform random systems.

We notice that in all the investigated CPAs the value $\rho\lambda^2 \approx 1$ appears to separate a highly structured eigenvalue distribution, where spatial correlations plays a dominant role, from a diffuse eigenvalue distribution with weaker correlations at low density.

The formation of spectral gaps in CPAs when increasing the optical density is best demonstrated in Figure 5 by the density of states (DOS) computed for all the investigated structures based on the imaginary part of the Green's matrix eigenvalues. In Fig. 5, we plot the DOS for all the structures at three representative optical densities, $\rho\lambda^2$ =100, 10, and 0.001, and plot them versus the normalized energy. Our numerical study indicates opening of gaps at values of the optical density $\rho\lambda^2 \gtrsim 10$. This density regime corresponds to a linear particle separation approximately equal to the wavelength, resulting in a strong diffractive response of the CPA structures. In particular, in Fig. 5(e), Eisenstein prime array has a gap near $(E - E_0)/\Gamma_0 = 1$, whereas in Fig. 5(h), Hurwitz prime array has multiple gaps near $(E - E_0)/\Gamma_0 =$ 0, 1, and 2. On the other hand, at the lowest optical density $\rho\lambda^2 = 0.001$ the scattering strength is too weak to open optical gaps in all the investigated structures, as demonstrated in Figs. 5(i-l). While this paper has primarily focused on $N \simeq 1000$ CPAs here, the results are more general and ready to be extended to scattering systems with larger N (see Fig. S4 of Supplemental Material [58]).

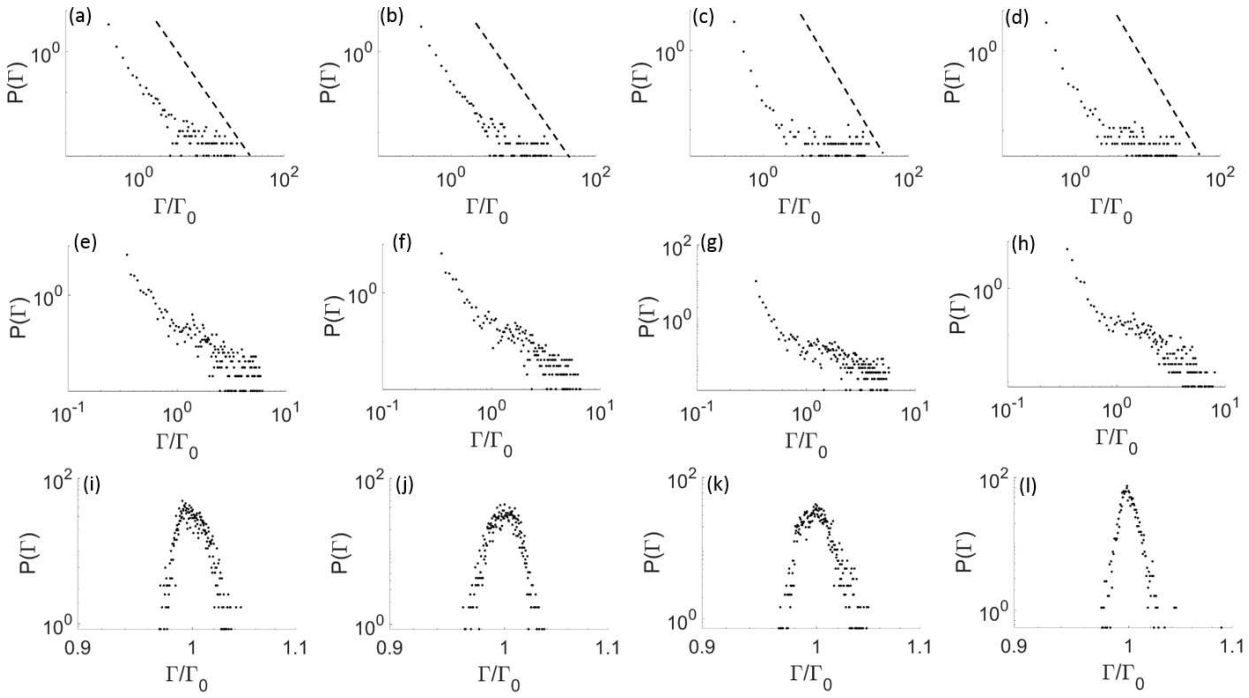

FIG. 7. . The decay rate statistics for ((a) Eisenstein prime, (b) Gaussian prime, (c) Hurwitz prime, (d) Lifschitz prime, at $\rho\lambda^2$=100; (e) Eisenstein prime, (f) Gaussian prime, (g) Hurwitz prime, (h) Lifschitz prime, at $\rho\lambda^2$=10.(i) Eisenstein prime, (j) Gaussian prime, (k) Hurwitz prime, (l) Lifschitz prime, at $\rho\lambda^2$=0.001.

SPECTRAL STATISTICS OF COMPLEX PRIMES

Level statistics provides important information about electromagnetic propagation in both closed and open systems, and from RMT one can to identify the wave transport regime (extended or localized) in closed systems. For open systems that are not random, level statistics remains not very well understood especially at low optical densities. In our previous work, we have applied the Green's matrix method to study open systems that are either random, or aperiodic, and have shown the transition from the absence to the presence of level repulsion as the optical density decreases [52]. In open systems the Green's matrix is non-Hermitian, so that for each Λ_i the nearest eigenvalue Λ_j is identified as the eigenvalue that minimizes the distance between the two eigenvalues in the complex plane $|\Delta\Lambda| = |\Lambda_i - \Lambda_j|$

In closed random systems, an established result from RMT predicts the suppression of level repulsion in the presence of localizes states [55, 59]. In this case two spatially separated, exponentially localized states hardly influence each other, so that distinct modes with infinitely close energies are possible. In the strong localization regime the distribution of level spacings is described by the Poisson distribution [59]:

$$p(s) \propto \exp(-s), \tag{5}$$

where we consider the nearest-neighbor level spacing normalized to the average spacing as $s = |\Delta\Lambda|/\langle|\Delta\Lambda|\rangle$. For inhomogeneous systems, as it is the case of CPAs, special care needs to be exercised in order to eliminate degenerate energy states caused by the geometrical symmetries inherent to the structure of the arrays.

In Fig. 6, we show the two most extreme cases (highest and lowest optical densities) of level spacing statistics for each of the four CPA structures. In particular, Figs. 6(a) to 6(d) show the first-neighbor level statistics of the Eisenstein prime, Gaussian prime, Lifschitz prime, and Hurwitz prime arrays, respectively, at $\rho\lambda^2 = 100$. The black lines in Figs. 6(a) to 6(d) are best fitting curves using a Poisson distribution model. The results demonstrate that level spacing with Poisson statistics has been achieved in the proposed CPAs for high optical densities, in complete analogy with the localization regime observed in uniform random media.

In contrast, a well-known result of RMT is the phenomenon of level repulsion in the extended regime of wave transport in closed systems [55, 59]. In open systems, the concept of eigenvalue repulsion can be generalized to non-Hermitian matrices. Indeed, for the Ginibre's ensemble of random matrices, the probability density function of normalized eigenvalue spacing is [59]

$$p(s) = \frac{3^4\pi^2}{2^7} s^3 \exp(-\frac{3^2\pi}{2^4} s^2), \tag{6}$$

which has been successfully applied to describe the statistical properties of eigenmodes in random optical me-

dia [60]. For all aperiodic media considered, we demonstrate the emergence of level repulsion, $i.e. P(0) = 0$, at low optical densities of $\rho\lambda^2 = 0.001$, as shown in In Figs. 6(e) to 6(h). However, in contrast to random media, the distribution of level spacing predicted by the Ginibre's ensemble in equation (6) (represented by dashed lines in Fig. 6) does not accurately describe the spectral statistics of CPAs. Instead, a good fit to the level statistics can be obtained only using the derivative of interpolation function, called critical cumulative probability, proposed in [61]:

$$I(s) = \exp[\mu - \sqrt{\mu^2 + (A_c s)^2}], \qquad (7)$$

where $I(s)$ is the cumulative level spacing distribution function, μ and A_c are fitting parameters. The fit of our data using this model is shown by the black lines in Figs. 6(e) to 6(h). The critical statistics model has been introduced to account for the level spacing at the Anderson transition in random media [61], where the wavefunctions feature multifractal scaling, and it has been proposed as a third universal level statistics valid at the Metal Insulator Transition (MIT) of aperiodic media.

Our findings demonstrate the applicability of critical statistics to the weakly scattering regime of CPAs. Indeed, the critical nature of the CPAs level spacing statistics can be traced back to their singular-continuous spectra that support critically localized eigenmodes with self-similar scaling at all optical densities. Differently from random media, where criticality is only achieved at the localization threshold, which occurs for a specific optical density in 3D, the critical behavior of CPAs occurs for a broader range of optical densities for planar, weakly scattering systems, and it is inherent to the fractal nature of their geometries and critical eigenmodes.

In Fig. 7 we show the decay rate statistics $P(\Gamma)$ for different CPAs and for for three distinct values of the optical density, where decay rates were obtained form the Green's matrix eigenvalues, $\Gamma/\Gamma_0 \approx Re\Lambda + 1$. [40] In particular, in Figs. 7(a-d) we plot the statistics of the normalized decay rates in a double-logarithmic scale, for the four prime-based aperiodic arrays at the highest optical density $\rho\lambda^2 = 100$. In this regime, we have conclusively found that the data follow a linear decay, which unveils an algebraic power law scaling $P(\Gamma) \simeq 1/\Gamma$. This power law behavior of the decay rate statistics, which has been reported in disordered systems [41, 46], is a result of multiple scattering [46]. Figures 7(a-d) indicate that the power law of $P(\Gamma) \sim \Gamma^{-1}$ also occurs for more general open aperiodic systems such as the CPAs for high optical densities ($\rho\lambda^2 = 100$). As it occurs in random systems [41], the range of this algebraic decay increases for increasing optical densities for which multiple scattering effects are stronger, as it can be seen by comparing Figs 7(a-d) with Figs 7(e-h), for which the optical density is lower, ($\rho\lambda^2 = 10$). Finally we note that, differently from uniformly random systems, the tails with very large decay rate in the statistics of CPAs shown in Figs. 7(a) to 7(d) do not feature any prominent peak due to Dicke superradiant modes, which would manifest as a peak at $P(\Gamma)$ at $\Gamma = 2\Gamma_0$) with IPR=0.5 [62, 63]. This result, together with the absence of proximity resonances with small decay rates unveiled in Fig. 3, show that collective effects involving pair of scatterers (subrandiance and superradiance), do not occur in the investigated CPAs. We believe that this behavior can be attributed to the highly correlated nature of CPAs, which prevents the formation of such modes.

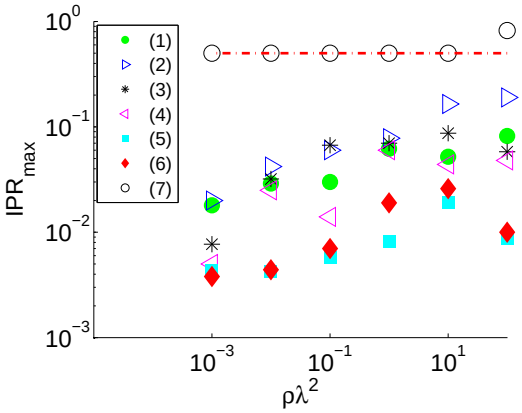

FIG. 8. (Color online) A comparison of maximum IPR values among (1) Eisenstein prime, (2) Gaussian prime, (3) Lifschitz prime, and (4) Hurwitz prime arrays, at each representative optical density. (5) square, (6) triangular and (7) uniform random arrays are included for references. The red dashed line indicate the proximity resonance of two particles with IPR = 0.5.

SPATIAL DISTRIBUTION OF EIGENSTATES

In order to further understand the spatial distribution of eigenmodes in aperiodically ordered structures, in Fig. 8 we show the maximum IPR value among all CPA eigenstates for different values of the optical density. For comparison, we also show the results obtained for a uniform random array of dipoles as well as for periodic square and triangular arrays. We have found that among all the investigated geometries the uniformly random array support eigenstates with the largest IPR values for all optical densities considered, as shown in Fig. 8. Indeed, these modes with largest $IPR = 0.5$ correspond to proximity resonances that involve only two neighboring particles and, as Fig. 8 reveals, can occur even for weakly scattering systems (low optical densities) [40]. Figure 8 demonstrates that these proximity resonances cannot be supported by CPAs under the conditions investigated. Besides, the largest values of IPR for CPAs are significantly larger than the corresponding ones of periodic arrays of dipoles. Based on the value of maximum IPR,

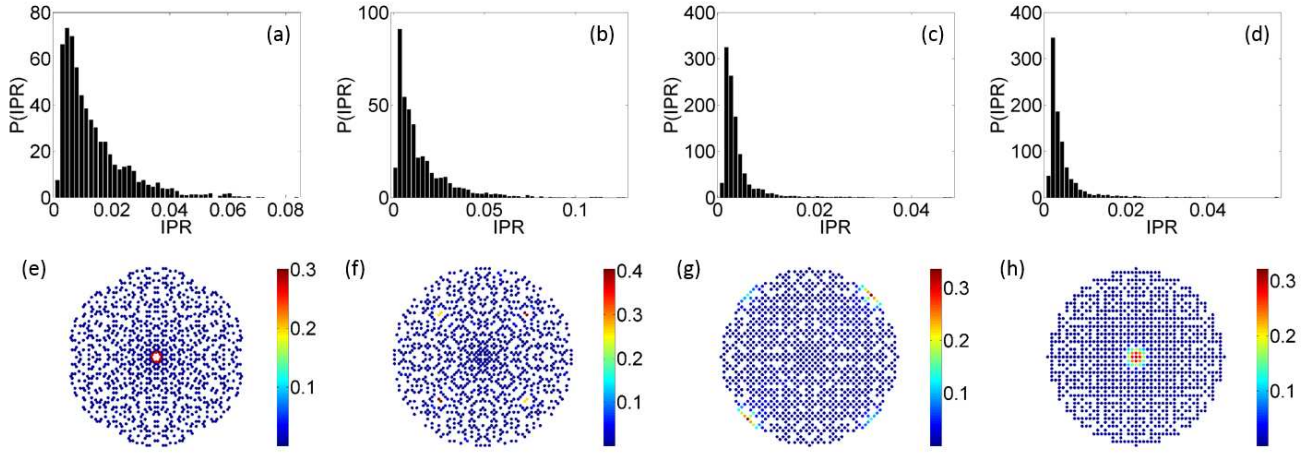

FIG. 9. (Color online) The IPR statistics for (a) Eisenstein prime, (b) Gaussian prime, (c) Hurwitz prime, (d) Lifschitz prime, at $\rho\lambda^2 = 100$; The mode with the highest IPR values are for each of the structures at this density are shown respectively from (e) to (h).

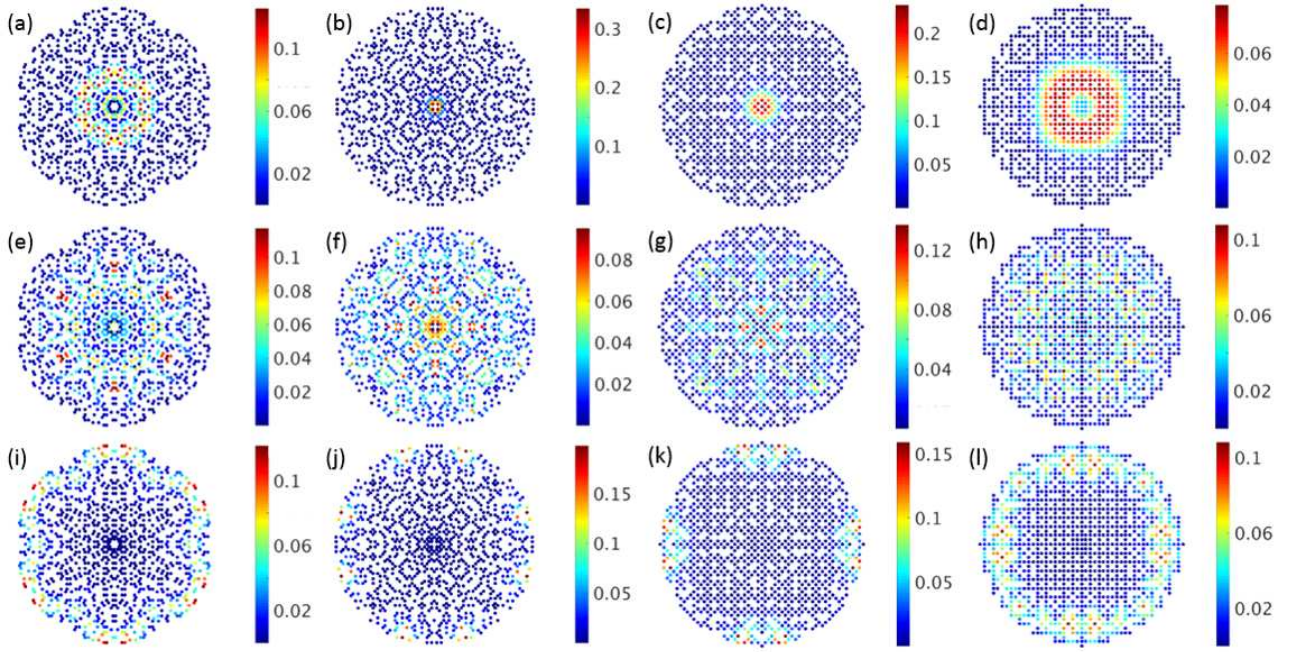

FIG. 10. (Color online) At $\rho\lambda^2 = 10$, (a) to (d) are the most localized (highest associated IPR value) eigenmode for Eisenstein prime, Gaussian prime, Hurwitz prime and Lifschitz prime arrays, respectively. (e) to (h) are corresponding structure's critical mode, which has the lowest IPR and small ReΛ (low decay rate). (i) to (l) are spectral-gap edge-modes of each corresponding structure.

we can estimate the number of particles over which the most spatially localized states are distributed.

In particular, at high optical densities, Efimov resonances [64], typically distributed over few dipoles, are more likely to occur in structures such as Eisenstein prime and Gaussian prime arrays.

In Figs. 9(a) to 9(d) the statistical distributions of IPRs are shown for CPAs in the strongly scattering regime, achieved at the largest optical density considered, $\rho\lambda^2 = 100$. It can be seen that the IPR distributions for Eisenstein prime and Gaussian prime arrays are considerably broader than the ones of the corresponding Hurwitz and Lifschitz primes structures. This result reflects the fact Hurwitz and Lifschitz prime arrays are much more regularly distributed in real space than the Eisenstein and Gaussian prime arrays, consistent with

the results for the Integrated Intensity Function shown in Fig. 2. Figures 9(a) to 9(d) also confirm that the probability of finding Efimov resonances, spatially localized over a small number M of scattering particles (with corresponding larger IPRs $\simeq 1/M$), is smaller for more regular CPAs, such as the Hurwitz and Lifschitz primes arrays. In Figs. 9(e-h) we show the intensities of the eigenvectors with largest IPR at the positions' of the scattering particles at optical density $\rho\lambda^2 = 100$ for different CPAs. The spatial distribution of the mode with largest IPR strongly depends on the particular spatial structure of the CPA in the real space. For instance, in the Eisenstein and Lifschitz prime arrays the mode with largest IPR is highly localized over a small cluster of dipoles in the center of structure, as Fig. 9(e) and (h) reveal. On the other hand, Fig. 9(g) demonstrates that for the Hurwitz prime array the highest-IPR eigenstate is symmetrically localized at the edge of the structure over T-shaped particle clusters.

In Fig. 10 we provide a more complete survey of the spatial extent of distinctive eigenstates that can be supported by different CPAs, namely the one with highest-IPR (panels (a) to (d)), the critical modes (panels (e) to (h)), and the ones localized at the edge of the structures (panels (i) to (l)) at $\rho\lambda^2 = 10$. Again, the spatial distribution of intensities of the highest-IPR mode crucially depends on the particular structure of the CPA in the real space. Indeed, Figs. 10 (a) to (d) demonstrate that, for a given optical density, the highest-IPR mode may be either extremely localized at the center of the array, as it is the case of Gaussian prime array, or more radially spread around the center of the structure, as in the Lifschitz prime array. The critical modes, which have been recently identified as the ones with long-lived resonances (small decay rates) with low IPR values [52], are depicted in Figs. 10(e-f). These modes, which are spatially extended over the whole array, are unique to deterministic aperiodic systems and cannot be supported by either random or periodic systems. Figs. 10(e-h) unveil the very rich spatial distribution and distinctive critical nature of eigenmodes for all CPAs considered. Finally, we also discovered in the CPAs mode spectrum long-lived modes that are spatially localized close to the edge of the structures, as shown in Figs. 10(i-l). Such surface-localized modes could be analogous to the recently discovered topological edge-states in quasiperiodic systems [29]. However, further studies beyond the scope of this work are needed to established the exact physical nature of edge-states in the investigated CPAs.

CONCLUSIONS

In conclusion, we have investigated the structural, spectral and localization properties of aperiodic arrays generated from the distribution of prime numbers in complex quadratic fields (Eisenstein, Gaussian) and quaternion rings (Hurwitz, and Lifschitz primes arrays) and studied their distinctive scattering resonances using the vector Green's matrix method. We systematically study the Fourier spectra, the eigenvalue distribution of the Green's matrix, the Density of States, level spacing distribution, the decay rate statistics, and the spatial extent of eigenmodes in all these structures. Our findings demonstrate several unique spectral properties, such as the absence of level repulsion for strongly scattering systems, critical level statistics, and the existence of critical modes, extended fractal modes with long lifetime that cannot be supported by either random and periodic systems. From the distribution of eigenvalues of Green's matrix in the complex plane, we are able to predict the existence spectral gaps. Our results unveil the importance of aperiodic correlations for the engineering of novel gapped photonic structures that support far richer spectral properties compared to traditional periodic and random media.

ACKNOWLEDGMENTS

This work was partly supported by the Army Research Laboratory through the Collaborative Research Alliance (CRA) for MultiScale Multidisciplinary Modeling of Electronic Materials (MSME) under Cooperative Agreement Number W911NF-12-2-0023. We thank The F.A.P. thanks the Royal Society-Newton Advanced Fellowship (Grant no. NA150208), CNPq, and FAPERJ for financial support.

* Corresponding author: dalnegro@bu.edu

[1] D. Wiersma, Nature Photonics **7**, 188 (2013).
[2] A. Lagendijk, B. A. van Tiggelen, and D. S. Wiersma, Phys. Today **62**, 24 (2009).
[3] M. Senechal, *Quasicrystals and Geometry* (Cambridge University Press, 1995).
[4] M. Kohmoto and L. P. Kadanoff, Phys. Rev. Lett. **50**, 1879 (1983).
[5] R. Merlin, K. Bajema, R. Clarke, F. Y. Juang, and P. K. Bhattacharya, Phys. Rev. Lett. **55**, 1768 (1985).
[6] M. Kohmoto, B. Sutherland, and K. Iguchi, Phys. Rev. Lett. **58**, 1987 (2436).
[7] E. Maci, Rep. Prog. Phys. **69**, 397 (2006).
[8] E. Maciá, *Aperiodic Structures in Condensed Matter: Fundamentals and Applications* (CRC Press Taylor and Francis: Boca Raton, FL, USA, 2009).
[9] E. Maciá, Rep. Prog. Phys. **75**, 036502 (2012).
[10] L. D. Negro, *Optics of Aperiodic Structures: Fundamentals and Device Applications* (Pan Stanford Publishing: Singapore, 2014).
[11] W. Steurer and D. Sutter-Widmer, J. Phys. D Appl. Phys. **40**, R229 (2007).

[12] L. D. Negro and N. N. Feng, Opt. Express **15**, 14396 (2007).
[13] C. Forestiere, G. Miano, G. Rubinacci, and L. D. Negro, Phys. Rev. B **79**, 085404 (2009).
[14] C. Forestiere, G. Miano, S. V. Boriskina, and L. D. Negro, Opt. Express **17**, 9648 (2009).
[15] A. E. Ostfeld and D. Pacifici, Appl. Phys. Lett. **98**, 113112 (2011).
[16] L. D. Negro and S. V. Boriskina, Laser Photonics Rev. **6**, 178 (2012).
[17] Z. V. Vardeny, A. Nahata, and A. Agrawal, Nat. Photonics **7**, 177 (2013).
[18] P. Barthelemy, J. Bertolotti, and D. S. Wiersma, Nature **453**, 495 (2008).
[19] S. Abe and H. Hiramoto, Phys. Rev. A **36**, 5349 (1987).
[20] R. Ketzmerick, K. Kruse, and T. G. S. Kraut, Phys. Rev. Lett. **79**, 1959 (1997).
[21] L. D. Negro, C. J. Oton, Z. Gaburro, L. Pavesi, P. Johnson, A. Lagendijk, R. Righini, M. Colocci, and D. S. Wiersma, Phys. Rev. Lett. **90**, 055501 (2003).
[22] L. D. Negro and S. Inampudi, Sci. Reports **7**, 2259 (2017).
[23] M. Kohmoto, B. Sutherland, and C. Tang, Phys. Rev. B. **35**, 1020 (1987).
[24] E. Maciá and F. Domínguez-Adame, Phys. Rev. Lett. **76**, 2957 (1996).
[25] S. Boriskina and L. D. Negro, Opt. Express **16**, 18813 (2008).
[26] J.-K. Yang, S. V. Boriskina, H. Noh, M. J. Rooks, G. S. Solomon, L. D. Negro, and H. Cao, Appl. Phys. Lett. **97**, 223101 (2010).
[27] S. Boriskina and L. D. Negro, Opt. Express **16**, 12511 (2008).
[28] E. L. Albuquerque and M. G. Cottam, Phys. Rep. **376**, 225 (2003).
[29] M. A. Bandres, M. C. Rechtsman, and M. Segev, Phys. Rev. X **6**.
[30] F. Baboux, E. Levy, A. Lemaitre, C. Gmez, E. Galopin, L. L. Gratiet, I. Sagnes, J. B. A. Amo, and E. Akkermans, Phys. Rev. B **95**, 161114(R) (2017).
[31] E. Levy and E. Akkermans, Eur. Phys. J. Special Topics **226**, 1563 (2017).
[32] W. Gellerman, M. Kohmoto, B. Sutherland, and P. C. Taylor, Phys. Rev. Lett. **72**, 633 (1994).
[33] M. Dulea, M. Johansson, and R. Riklund, Phys. Rev. B **45**, 105 (1992).
[34] L. D. Negro, J. H. Yi, V. Nguyen, Y. Yi, J. Michel, and L. C. Kimerling, Appl. Phys. Lett. **86**, 261905 (2005).
[35] S. V. Boriskina, A. Gopinath, and L. D. Negro, Opt. Express **16**, 18813 (2008).
[36] T. Apostol, *Introduction to Analytic Number Theory, 2nd Edition* (Springer-Verlag NY, 1976).
[37] G. H. Hardy and E. M. Wright, *An introduction to the theory of numbers, 6th Edition* (Oxford University Press, Oxford, 2006).
[38] M. Wolf, Physica A **241**, 493 (1997).
[39] K. W. P. Bak, C. Tang, Phys. Rev. Lett. **59**, 381 (1987).
[40] M. Rusek, J. Mostowski, and A. Orlowski, Phys. Rev. A **61**, 022704 (2000).
[41] F. A. Pinheiro, M. Rusek, A. Orlowski, and B. A. van Tiggelen, Phys. Rev. E **69**, 026605 (2004).
[42] F. A. Pinheiro and L. C. Sampaio, Phys. Rev. A **73**, 013826 (2006).
[43] F. A. Pinheiro, Phys. Rev. A **78**, 023812 (2008).
[44] A. Goetschy and S. E. Skipetrov, EPL **96**, 34005 (2011).
[45] S. E. Skipetrov and A. Goetschy, J. Phys. A: Math. Theor. **44**, 065102 (2011).
[46] A. Goetschy and S. E. Skipetrov, Phys. Rev. E **84**, 011150 (2011).
[47] E. Gethner, S. Wagon, and B. Wick, American Mathematical Monthly **105** (1998).
[48] I. Vardi, Experimental Mathematics **7** (1998).
[49] T. Tao, J. Anal. Math. **99** (2006).
[50] A. Hurwitz, *Vorlesungen uber die Zahlentheorie der Quaternionen* (Berlin: J. Springer, 1919).
[51] J. H. Conway and D. A. Smith, *On quaternions and octonions: their geometry, arithmetic, and symmetry* (A. K. Peters: Natick, Massachusetts, USA:).
[52] L. D. Negro, R. Wang, and F. A. Pinheiro, Crystals **6**, 161 (2016).
[53] E. Maciá, *Aperiodic Structures in COndensed Matter* (CRC Press: Boca Raton, FL, 2009).
[54] F. Dyson, Notices of the AMS **56** (2009).
[55] M. L. Mehta, *Random Matrices* (Elsevier, Amsterdam, 2004).
[56] A. Christofi, F. A. Pinheiro, and L. D. Negro, Opt. Lett. **41**, 1933 (2016).
[57] A. Lagendijk and B. A. van Tiggelen, Resonant Multiple Scattering of Light **270**, 143 (1996).
[58] "See supplemental material at [url will be inserted by publisher] for eigenvalue distributions at various optical densities.".
[59] F. Haake, *Quantum Signitures of Chaos, Third Revised and Enlarged Edition* (Springer-Verlag Berlin Heidelberg, 2010).
[60] S. E. Skipetrov and I. M. Sokolov, Physical Review Letters **114**, 053902 (2015).
[61] I. K. Zharekeshev and B. Kramer, Phys. Rev. Lett. **79** (1997).
[62] E. Akkermans and A. G. andR. Kaiser, Phys. Rev. Lett. **101**, 103602 (2008).
[63] R. H. Dicke, Phys. Rev. **93**, 99 (1954).
[64] V. Efimov, Phys. Lett. B **33**, 563 (1970).